

Supplementary Materials

FDNIRS-DCS Device

DCS and FDNIRS detectors acquire data in parallel, with the DCS laser at 850 nm always on and the eight FDNIRS lasers (wavelengths ranging from 670 to 830 nm) turned on sequentially in rapid succession (10 Hz cycle with each laser on for 12 ms) (1). In patients #1, 5 and 8, the DCS operated at 2 Hz. In all other patients the device operating software was updated, and FDNIRS-DCS was run at 10 Hz. Crosstalk between the DCS and FDNIRS components is eliminated by optical filters in front of the detectors. To comply with the American National Standards Institute's standards (ANSI), the DCS laser power was set at below 34 mW, the FDNIRS laser power between 2-3 mW, and the light at the probe was diffused over an area > 1mm. Measurements in patient #2 were done with a DCS-only device with the same design and laser as the DCS portion of the MetaOx system, but with only 4 photon-counting modules, as used in a study by Selb et al (2).

Probe

Light sources and detectors from the device were connected via fiber optics to a soft rubbery 3D printed probe attached to the patient's head. All the fibers at the probe end were terminated with prisms to allow for a low probe profile. For light transmission to the patient, we used a single fiber cable that included the fiber bundle from the FDNIRS lasers and a 200 mm multimode fiber from the DCS laser. One single mode fiber located at 5 mm from the source collected the short separation DCS light. 4 fiber bundles at 2, 2.5, 3 and 3.5 cm distances from the source collected photons back to the FD-NIRS detectors. Some of these bundles also included DCS single mode detection fibers for a colocalized acquisition (Figure 1 in Manuscript).

FDNIRS Data Analysis

We used custom MATLAB code for all data analysis. In preprocessing, we smoothed the 10 Hz FDNIRS AC and phase shift using a 50-point averaging window, down-sampling to 0.2 Hz. The FDNIRS data had interference from the hospital oximeter and affected data were removed during preprocessing. In two patients the interference was particularly strong, hence we had to discard large sections of the raw data and only recovered discontinuous SO₂ measurements. The hospital INVOS cerebral oximeter employs 730 nm and 810 nm LEDs switched on and off at < 30 Hz, while our FDNIRS employs 8 wavelengths turned on in sequence at 10 Hz per cycle. The light cross-talk of the two devices results in spurious peaks in the FDNIRS signal, which appear at different wavelengths and different times throughout the data collection. By using Fourier analysis, we found and discarded contaminated data segments, typically lasting less than 1 minute. We also interpolated across the discarded periods to obtain continuous time traces. The raw signal for one

of these patients is shown in Figure 6. In patients #4 and #12, our probe was so close to the hospital oximeter's probe and the interference was so strong that we could not recover a continuous signal, but rather only segments. The strength of this interference is shown in Figure 7.

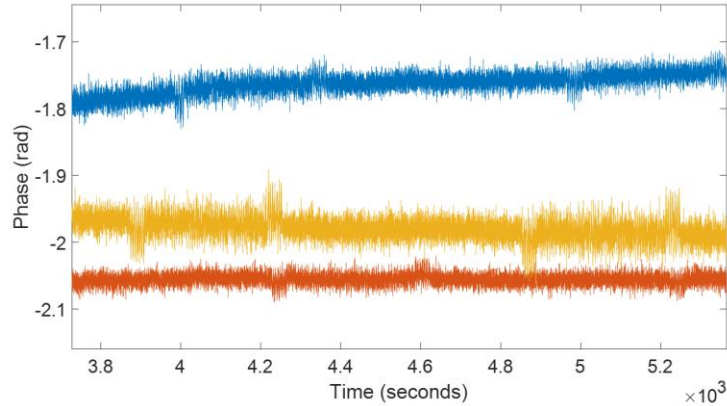


Fig 6: Interference of the INVOS with the FDNIRS raw phase data on patient #6. The figure shows the phase signal at 3 wavelengths for one detector with no preprocessing. The small jumps in the raw signal are due to the repetitive interference caused by the 30 Hz light modulation of the INVOS oximeter. Each jump is roughly 30-50 seconds wide.

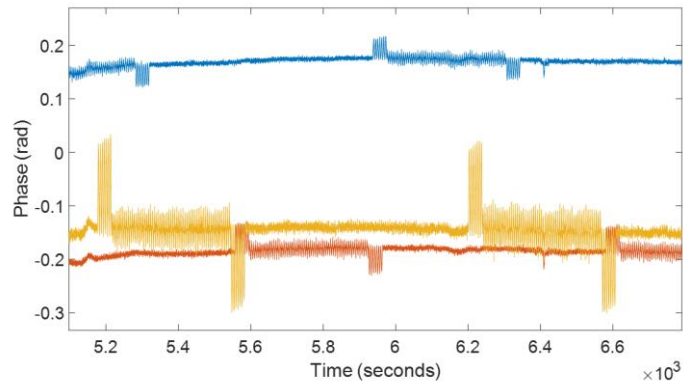


Fig 7: FDNIRS phase data from patient #12, one of the two patients where the interference was so strong and overlapping at different wavelengths that we could only recover sections of FDNIRS data. Each interference section is ~7 minutes wide, making potential interpolation infeasible. For these patients, rather than linearly interpolating, we removed interference sections leaving gaps in the data before further analysis.

After preprocessing the raw data, we used the frequency domain multi-distance method (3) to compute the optical properties of the measured tissue with a minimum of 5 out of the 8 wavelengths. At each wavelength, the AC and phase shift slopes versus distance were used to quantify the absorption and scattering coefficients, μ_a and μ_s' , respectively. After calculating μ_a and μ_s' at all wavelengths, we computed the oxy, deoxy and total hemoglobin concentrations, as well as the hemoglobin oxygen saturation (SO_2) assuming a water fraction in tissue of 0.75.

DCS Analysis

During preprocessing, the DCS intensity autocorrelation functions (g_2) were smoothed using a 10-point averaging window for patients #1, 5 and 8 (acquired at 2 Hz), and a 50-point window for all other patients (acquired at 10 Hz) to achieve a final sampling rate of 0.2 Hz in all patients. We further smoothed the g_2 with a 5-point moving average to improve signal to noise ratio.

We analyze the DCS data using the semi-infinite medium boundary condition for correlation diffusion equation (3). In all subjects we report BF_i at 25 mm separation except for patient #12, for which we only had the measure at 30 mm. Optical properties at 850 nm are needed to calculate blood flow index (BF_i). For 6 patients (#2-4, 6-7, 9-10) we used the optical properties measured with the FDNIRS by extrapolating absorption and reduced scattering spectra at 850 nm. For all the other patients, since we did not have FDNIRS measurements, we used average optical properties measured in the above patients, specifically, we used $\mu_a = 0.12$ and $\mu_s' = 8.94$. In the 6 subjects with measured optical properties we also calculated BF_i using fixed optical properties and confirmed that there were no significant changes in the estimated flow relative changes.

Quantification of CBF_i changes with circulatory arrests

We quantified the CBF_i at CAs by calculating the average BF_i changes during the CA period with respect to that of a pre-CA period for each patient. The duration of the pre-CA period was defined manually as a 1- to 10- minute window immediately before the CA onset during which BF_i , SO_2 and systemic physiology were stable. The CBF_i changes during HCA were calculated by averaging BF_i from 90 seconds after CA start until the stop time. The 90-second delay was used to discard any artifacts at the beginning of the procedure. We measured the CBF_i overshoot at reperfusion times by averaging the values at the highest reperfusion peaks (there were multiple peaks in some cases where the surgeon asked to have the pump started and stopped several times) and comparing them to the settled CBF_i value, found by averaging a several-minute window after the overshoot.

Quantification of SO_2 changes through circulatory arrests

For the patients with FDNIRS measurements, we quantified SO_2 drops by averaging one-minute pre-CA and the one-minute right before reperfusion.

Quantification of cerebral metabolic rate of oxygen and its relationship with temperature

To calculate oxygen consumption, we used the equation: $CMRO_{2i} = \frac{HGB}{MW_{Hb}} * CBF_i(SaO_2 - SO_2)$ (4), where HGB is the patient's hemoglobin concentration in the blood (units g/dL) and MW_{Hb} is the molecular weight of hemoglobin (65,400 g/Mol). HGB was collected at 30-minute intervals by the clinical team, and we linearly interpolated over the points to get a continuous variable. In all 6 patients, arterial oxygenation

(SaO₂) was maintained at 100% by the cardiopulmonary bypass during cooling and rewarming. As described above SO₂ was measured with the FDNIRS and CBF_i was calculated using actual optical properties.

For each patient, CMRO_{2i} averages for cooling and rewarming periods were calculated separately. We averaged CMRO₂ values over 2°C associated with up to seven evenly spaced temperature windows, from 20.5°C to 34.5°C. We normalized each patient’s CMRO_{2i} values with respect to the average CMRO_{2i} in the window between 34.5-36.5°C, taken during each patient’s rewarming period. Data with significant artifacts in CBF_i caused by CPB flow rate adjustments were excluded from calculations. To estimate the CMRO_{2i} relationship with temperature, we fit a linear regression for all patients’ normalized CMRO_{2i} (log scale) with respect to the mean temperature windows.

Other parameters of interest at circulatory arrests

Perfusion Group	CBF _i Drop from baseline (%)	CBF _i Overshoot (%)	SO ₂ Baseline (FDNIRS, %)	SO ₂ Drop (FDNIRS, %)	INVOS Left Baseline (%)	INVOS Left Drop (%)	INVOS Right Baseline (%)	INVOS Right Drop (%)	MAP Baseline (mmHg)	MAP Drop (%)
HCA-Only	94.6 ± 1.0%	240 ± 50	59 ± 7%	18 ± 4%	77 ± 7%	27 ± 10%	70 ± 0.6%	26 ± 10%	64 ± 4	79 ± 3%
RCP	91 ± 3%	250 ± 70	70.2%*	13%*	95%*	7%*	95%*	12%*	64 ± 7	75 ± 10%
ACP	-12 ± 28%	N/A	59 ± 14%	3.4 ± 1.8%	91 ± 3%	10 ± 11%	83 ± 7%	2 ± 6%	73 ± 28	24 ± 29%

Table 2: Group-level quantification of CBF_i, SO₂, INVOS and MAP behavior with circulatory arrests. Baseline is equivalent to Pre-CA window defined for CBF_i and SO₂ defined above. CBF_i overshoot is calculated by comparing the maximum value reached at reperfusion with the mean value reached 1-3 minutes after reperfusion. *Standard deviation not estimated since ≤ 2 patients had this measurement.

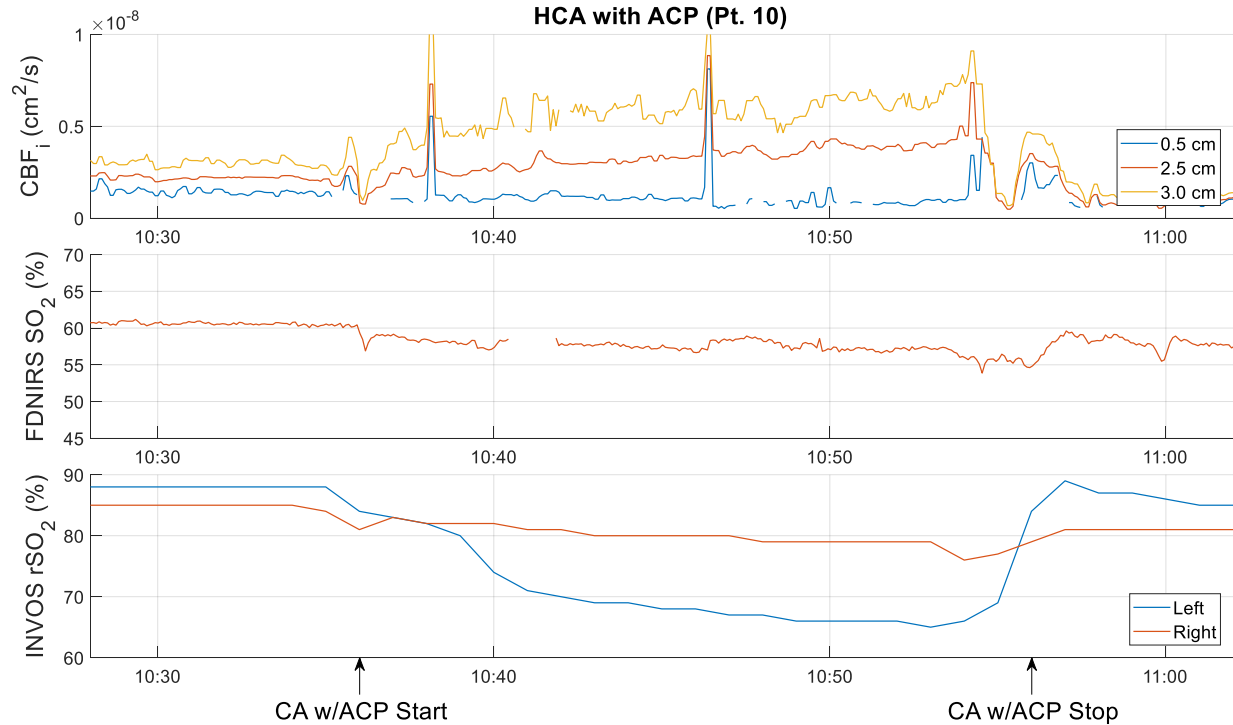


Fig 8: CBF_i , SO_2 and INVOS rSO_2 time-traces around CA for patient #10 during antegrade cerebral perfusion. CBF_i and FDNIRS are measured on the right side whereas INVOS has bilateral measurements. Note that although the right side FDNIRS and INVOS oxygen saturation report relatively steady levels, the left INVOS rSO_2 drops throughout the CA, suggesting no blood flow delivery on that hemisphere as in the RCP or HCA-only cases. This may be caused by an incomplete Circle of Willis. CBF_i measured on the right side supports this hypothesis since increasing perfusion pressure from the clinical team only served to increase CBF_i through CA, with the long separations CBF_i increasing to over 200% of the pre-CA levels. Artifacts in CBF_i through CA are from a clinician pressing on the probe mid-procedure.

References

1. Carp SA, Farzam P, Redes N, Hueber DM, Franceschini MA. Combined multi-distance frequency domain and diffuse correlation spectroscopy system with simultaneous data acquisition and real-time analysis. *Biomedical optics express*. 2017 Sep;8(9):3993–4006.
2. Selb J, Wu K-C, Sutin J, Lin P-YI, Farzam P, Bechek S, et al. Prolonged monitoring of cerebral blood flow and autoregulation with diffuse correlation spectroscopy in neurocritical care patients. *Neurophotonics*. 2018 Oct;5(4):45005.
3. Durduran T, Choe R, Baker WB, Yodh AG. Diffuse Optics for Tissue Monitoring and Tomography. *Reports on progress in physics Physical Society (Great Britain)*. 2010 Jul;73(7).
4. Roche-Labarbe N, Carp SA, Surova A, Patel M, Boas DA, Grant PE, et al. Noninvasive optical measures of CBV, StO_2 , CBF index, and $rCMRO_2$ in human premature neonates' brains in the first six weeks of life. *Human brain mapping*. 2010 Mar;31(3):341–52.